Master's Thesis

Impact of Air-Sea Interaction on the East Asian Summer Monsoon Simulation in Coupled Model Intercomparison Project 5 Models

Soheon Lee

Department of Urban and Environmental Engineering
(Disaster Management Engineering)

Graduate School of UNIST

2019

Impact of Air-Sea Interaction on the East Asian Summer Monsoon Simulation in Coupled Model Intercomparison Project 5 Models

Soheon Lee

Department of Urban and Environmental Engineering
(Disaster Management Engineering)

Graduate School of UNIST

Impact of Air-Sea Interaction on the East Asian Summer Monsoon Simulation in Coupled Model Intercomparison Project 5 Models

A thesis
submitted to the Graduate School of UNIST
in partial fulfillment of the
requirements for the degree of
Master of Science

Soheon Lee

12.05.2018
Approved by

Advisor
Dong-Hyun Cha

Impact of Air-Sea Interaction on the East Asian Summer Monsoon Simulation in Coupled Model Intercomparison Project 5 Models

Soheon Lee

This certifies that the thesis of Soheon Lee is approved.

12.05.2018

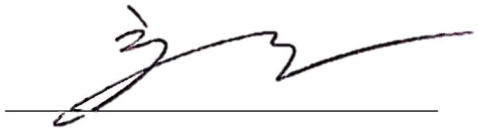

Dong-Hyun Cha

Ulsan National Institute of Science and Technology

Myong-In Lee

Ulsan National Institute of Science and Technology

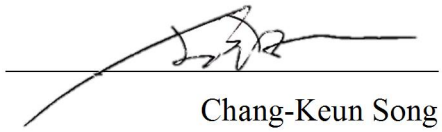

Chang-Keun Song

Ulsan National Institute of Science and Technology

Abstract

A comprehensive study on the relationship between global climate models (GCMs)' performances simulating the western North Pacific (WNP) air-sea interaction and reproducing the East Asian summer monsoon (EASM) is conducted. Among the GCMs participated in the third phase of the Coupled Model Intercomparison Project (CMIP3) and GCMs participated in the CMIP5, good models and bad models are selected, according to the performance simulating relations between the WNP sea surface temperature (SST) and precipitation. In comparison with CMIP3 models, CMIP5 models have improved in terms of simulating the unique property of the western North Pacific (WNP), regarding the air-sea interaction – the strong atmospheric forcing on the ocean. Among the CMIP5 models, good performing models are determined to be more capable of predicting EASM than bad performing models are. The good model ensemble simulates proper force-response mechanism for the WNP and East Asia, that is mainly due to the synoptic scale atmospheric conditions, and less effect of the local SST. The good models are also better than the bad models generating realistic temporal evolution of EASM as well as the spatial distribution. Bad models' defects are analyzed to result from distorted synoptic geopotential height and wind fields, inducing unrealistic moisture supply and convection due to the exaggerated SST forcing. The features are adequately simulated in the good models. The performance of CMIP5 good models and CMIP5 bad models were especially different in simulating monsoon system in the strong EASM years. According to the model results, precipitation is anticipated to increase in the early future and late future in the East Asia. However, predicted rainfall intensity and spatial pattern were different in CMIP5 good models and CMIP5 bad models. CMIP5 bad models tend to estimate more precipitation than CMIP5 good models do. Projected results are different from each other according to the members of GCMs. Thus, for better future projection, proper model selection should be regarded as important factor.

Keywords Air-sea interaction · EASM · Precipitation · CMIP5 · Intercomparison

Contents

List of Figures

List of Tables

Chapter I

Introduction

The role of monsoon circulation is essential all over the world; especially East Asia summer monsoon (EASM) is one of the most critical components of East Asia's general circulation system (Lau et al., 2000). The EASM is a broad scale summer monsoon over East Asia and the western North Pacific (WNP) region. It covers China, Korean Japan, and surrounding ocean basins. The EASM often accompanies various extreme weather events such as heat wave, drought, heavy rainfall, or floods that are hard to forecast in advance. In this context, proper preparations for the disasters caused by abnormal weather and climate require better model accuracy simulating EASM. A noticeable feature of this monsoon system is the broad range of precipitation that varies in duration, areal extent, and intensity. One of the most important factors for generating this convection on the ocean is the air-sea interaction – the two-tier energy exchange between the atmosphere and the ocean (Tompkins, 2001). This mutual interaction denotes that the ocean not only controls atmospheric conditions but also gets influenced by the atmosphere.

It is well known that sea surface temperature (SST) represents oceanic activity and precipitation is representative of the atmosphere. The air-sea interaction, therefore, can be explained by the relationship between SST and precipitation. SST plays a crucial role in driving atmospheric processes when SST is high enough, for the warm SST increases surface water evaporations, mean atmospheric ascents, and thus low-level convergences. These phenomena tend to induce much more convective precipitations on the region. Thus, in the tropics and subtropics, SST anomaly and precipitation are positively correlated. On the contrary, Activities driven by the atmosphere occur in the region with lower SST as the impact of the atmosphere on SST is greater than the effect of SST on the atmosphere. When precipitation occurs, decreased solar radiation to the sea surface leads to decreased SST. Also, surface wind can cool SST by increasing ocean boundary layer mixing (Cha et al. 2016). However, unlike the other ocean basin, the western North Pacific (WNP), often called as 'western Pacific warm pool', has a unique characteristic regarding the SST-precipitation relationship. Tompkins (2001) demonstrated that observed SST of WNP seems inversely proportional to precipitation, implying that the atmospheric condition forces the oceanic activity even with the remarkably high SST around 30 . If the warm SST does not decrease despite precipitation and the low-level wind in models, unreasonable positive feedback from the sea surface to precipitation will lead to unrealistic EASM prediction (Cha et al. 2016). To analyze this air-sea interaction and validate GCMs, Air-Sea interaction Index (ASI) is defined as the cross-correlation coefficient between precipitation and SST in this paper.

Lack of reproducing these aspects of air-sea interaction and ASI in global circulation models (GCMs) can be related to numerous errors in forecasting atmospheric phenomena. GCMs participated in the atmospheric model intercomparison project (AMIP) produced unrealistic precipitation variability of Asian-Pacific summer monsoon. One reason for the failure is neglecting air-sea interaction in the warm Indo-Pacific oceans (Gadgil and Sajani, 1998). Especially for the WNP, as air-sea interaction is different from other oceans, it is more critical. Wang et al. (2005) demonstrated that a major cause for rainfall-deficiencies of atmospheric general circulation models (AGCMs) is because atmospheric feedback to the ocean is not considered. AGCMs use prescribed SST just as a forcing. Generally, predictability is high over regions where precipitation and SST are positively correlated; but it is low over the regions with negative precipitation-SST correlation (Kumar et al., 2013). Due to its importance, air-sea interaction is of interest to many scientists. Various studies have proved that the performance of GCMs and regional climate models (RCMs) are improved when ocean models are coupled. For the boreal-summer intraseasonal oscillation (BSISO) and climatological intraseasonal oscillation (CISO) of the mean Asian summer monsoon, the air-sea coupled system allows more realistic mimicking than the atmosphere-only approach (Fu et al., 2002; Fu and Wang., 2004). In terms of RCM also, including an ocean mixed layer model into the regional Weather Research and Forecasting (WRF) model tends to improve the summer climate simulation over East Asia during 2000-2008 because the ocean model cools down SST and stabilizes the thermodynamic structure near the surface, reducing overestimated summer precipitation and weakened sub-tropical high (Kim and Hong, 2010). Cha et al. (2016) also demonstrated that SNURCM runs coupled with a slab ocean model (SOM), represented western North Pacific subtropical high (WNPSH), seasonal mean rainfall, and monsoon circulations more realistically than uncoupled runs.

The Coupled Model Intercomparison Project (CMIP) was established to study and intercompare climate representations made with coupled ocean-atmosphere-cryosphere-land GCMs (Meehl et al., 2000). As diverse ocean models are embedded in atmospheric models, they are expected to have more improved skills than the atmosphere-only global models do. The number of GCMs participated in each phase are increasing; their performances also have been enhanced compared with the previous version models. For example, mimicking climatological seasonal mean and interannual standard deviation fields of precipitation by the global models participated in the fifth phase of Coupled Model Intercomparison Project (CMIP5) got better greatly compared with CMIP3 models (Seo et al., 2013). Nevertheless, studies on the comparison of CMIP5 models against CMIP3 representing air-sea correlation in WNP are still required. Specific evaluations on the SST-precipitation relationship over the WNP-where the SST-precipitation correlation is most strongly negative among the tropical ocean-have not been documented yet (Lu and Lu, 2014). Moreover, the impact of performance simulating the

interaction on the achievement of down to earth EASM forecast should be analyzed more deeply. Therefore, the purpose of this study is to investigate the impacts of the performance reproducing western North Pacific (WNP) ASI on the simulation of the East Asian summer monsoon by CMIP5 models.

The arrangement of the paper is as follows. Section 2 describes the reslationship hetween precipitation and sea surface temperature in the wsetern north pacific. In section 3, study on the relatioship between the WNP air-sea interaction and the east asian summer monsoon prediction is conducted. Finally, section 4 summarizes the key findings.

Chapter II

Relationship between Precipitation and Sea Surface Temperature in the Western North Pacific

2-1. Datasets and Methods

A large ensemble of GCM data was selected from the 'Climate of the 20 century' experiment of WCRP CMIP3 (Meehl et al. 2007) and from the historical multi-model datasets from WCRP CMIP5 (Taylor et al. 2012). The available model outputs are from 20 models of CMIP3 and 44 models of CMIP5; they are all listed in Table 2.1. For the widest ensemble size, only one realization (run1 for CMIP3 and r1i1p1 for CMIP5) of each GCM was taken into account. Produced monthly SST, precipitation, geopotential height, and wind vectors are used. The observational and reanalysis datasets used in this study consist of followings: 1) the Global Precipitation Climatology Project (GPCP) (Adler et al., 2003) for monthly and daily precipitation data; 2) the National Centers for Environmental Prediction/Department of Energy (NCEP/DOE) R-2 data (Kanamitsu et al., 2002) for monthly SST, geopotential height, and wind vectors. All datasets are interpolated into a 2.5°×2.5° common grid resolution.

Cross-correlation coefficient between monthly mean precipitation and SST (also referred to as ASI) is calculated for the period of May-August (MJJA) from 1980 to 1999 to analyze the air-sea interaction in the WNP. To validate and compare CMIP5 models' EASM simulation, the analysis period is extended to 1979-2005 for higher reliability. To examine the overall performance of CMIP3 and CMIP5 models, the Taylor (2001) analysis is performed for reproduced ASI compared to the observed ASI. The Taylor skill score S is defined as

$$S = \frac{4(1+R)}{\left(\hat{\sigma}_f + 1/\hat{\sigma}_f\right)^2 (1+R_0)},$$

where R is the spatial correlation between simulated and observation, $\hat{\sigma}_f$ is the ratio of simulated and observed standard deviation, and R_0 is a possible maximum correlation (here set to 1). The skill score S, therefore, can evaluate both the normalized spatial standard deviation and pattern correlation simultaneously. According to the ASI-reproducing skill score, good-performing models and bad-performing models were selected and compared.

Table 2.1. a) CMIP3 and b) CMIP5 models and their corresponding institutions. Further information on the models used can be obtained from https://pcmdi.llnl.gov/mips/

a) CMIP3

Models	Institution
BCCR-BCM2.0	Bjerknes Centre for Climate Research
CNRM-CM3	Météo-France / Centre National de Recherches Météorologiques
CSIRO-Mk3.0	Commonwealth Scientific and Industrial Research Organization Atmospheric Research
ECHO-G	Meteorological Institute of the University of Bonn, Meteorological Research Institute of KMA, and Model and Data group.
FGOALS-g1.0	LASG / Institute of Atmospheric Physics
GFDL-CM2.0	US Dept. of Commerce / NOAA / Geophysical Fluid Dynamics Laboratory
GFDL-CM2.1	US Dept. of Commerce / NOAA / Geophysical Fluid Dynamics Laboratory
GISS-AOM	NASA / Goddard Institute for Space Studies
GISS-EH	NASA / Goddard Institute for Space Studies
GISS-ER	NASA / Goddard Institute for Space Studies
UKMO-HadCM3	Hadley Centre for Climate Prediction and Research / Met Office
UKMO-HadGEM1	Hadley Centre for Climate Prediction and Research / Met Office
INM-CM3.0	Institute for Numerical Mathematics
IPSL-CM4	Institut Pierre Simon Laplace
MIROC3.2(hires)	Center for Climate System Research (The University of Tokyo), National Institute for Environmental Studies, and Frontier Research Center for Global Change (JAMSTEC)
MIROC3.2(medres)	Center for Climate System Research (The University of Tokyo), National Institute for Environmental Studies, and Frontier Research Center for Global Change (JAMSTEC)
ECHAM5/MPI-OM	Max Planck Institute for Meteorology
MRI-CGCM2.3.2	Meteorological Research Institute
CCSM3	National Center for Atmospheric Research
PCM	National Center for Atmospheric Research

b) CMIP5

Models	Institution
ACCESS1.0	CSIRO (Commonwealth Scientific and Industrial Research Organisation, Australia), and BOM (Bureau of Meteorology, Australia)
ACCESS1.3	CSIRO (Commonwealth Scientific and Industrial Research Organisation, Australia), and BOM (Bureau of Meteorology, Australia)
BCC-CSM1.1	Beijing Climate Center, China Meteorological Administration
BCC-CSM1.1(m)	Beijing Climate Center, China Meteorological Administration
CanCM4	Canadian Centre for Climate Modelling and Analysis
CanESM2	Canadian Centre for Climate Modelling and Analysis
CCSM4	National Center for Atmospheric Research
CESM1-BGC	National Science Foundation, Department of Energy, National Center for Atmospheric Research
CESM1-CAM5	National Science Foundation, Department of Energy, National Center for Atmospheric Research
CESM1-FASTCHEM	National Science Foundation, Department of Energy, National Center for Atmospheric Research
CESM1-WACCM	National Science Foundation, Department of Energy, National Center for Atmospheric Research
CMCC-CESM	Centro Euro-Mediterraneo per I Cambiamenti Climatici
CMCC-CM	Centro Euro-Mediterraneo per I Cambiamenti Climatici
CMCC-CMS	Centro Euro-Mediterraneo per I Cambiamenti Climatici
CNRM-CM5	Centre National de Recherches Meteorologiques / Centre Europeen de Recherche et Formation Avancees en Calcul Scientifique
CSIRO-Mk-3-6-0	Commonwealth Scientific and Industrial Research Organisation in collaboration with the Queensland Climate Change Centre of Excellence
FGOALS-g2	LASG, Institute of Atmospheric Physics, Chinese Academy of Sciences; and CESS, Tsinghua University
FIO-ESM	The First Institute of Oceanography, SOA, China
GFDL-CM2.1	Geophysical Fluid Dynamics Laboratory
GFDL-CM3	Geophysical Fluid Dynamics Laboratory
GFDL-ESM2G	Geophysical Fluid Dynamics Laboratory
GFDL-ESM2M	Geophysical Fluid Dynamics Laboratory
GISS-E2-H-CC	NASA Goddard Institute for Space Studies
GISS-E2-H	NASA Goddard Institute for Space Studies
GISS-E2-R-CC	NASA Goddard Institute for Space Studies
GISS-E2-R	NASA Goddard Institute for Space Studies
HadCM3	Met Office Hadley Centre
HadGEM2-AO	Met Office Hadley Centre
HadGEM2-CC	Met Office Hadley Centre
HadGEM2-ES	Met Office Hadley Centre
INMCM4	Institute for Numerical Mathematics
IPSL-CM5A-LR	Institut Pierre-Simon Laplace
IPSL-CM5A-MR	Institut Pierre-Simon Laplace
IPSL-CM5B-LR	Institut Pierre-Simon Laplace
MIROC4h	Atmosphere and Ocean Research Institute (The University of Tokyo), National Institute for Environmental Studies, and Japan Agency for Marine-Earth Science and Technology
MIROC5	Atmosphere and Ocean Research Institute (The University of Tokyo), National Institute for Environmental Studies, and Japan Agency for Marine-Earth Science and Technology
MIROC-ESM-CHEM	Japan Agency for Marine-Earth Science and Technology, Atmosphere and Ocean Research Institute (The University of Tokyo), and National Institute for Environmental Studies
MPI-ESM-LR	Max Planck Institute for Meteorology
MPI-ESM-MR	Max Planck Institute for Meteorology
MPI-ESM-P	Max Planck Institute for Meteorology
MRI-CGCM3	Meteorological Research Institute
NorESM1-M	Norwegian Climate Centre

2-2. Model Performances Simulating the WNP Air-Sea Interaction by CMIP3 and CMIP5 models

The ASI reproduced by GCMs participated in CMIP3 and CMIP5 are analyzed in this section. To understand air-sea interactions on the WNP, observed ASI is first studied (Figure 2.1(a)). ASI is negative in most area of the WNP. Not only the mid-latitude area near 30^{o}N around the Korean peninsula but also low-latitude regions in the vicinity of the Philippines have noticeable negative ASI. Especially near the west of the Philippines and over the South China Sea, there is a core region (10-30^{o}N, 110-135^{o}E) with strong negative ASI signals with the coefficient of larger than 0.5. It is where the atmospheric forcing on the sea is much stronger than the impacts of the ocean to the atmosphere. This negative ASI is then reversed to positive in the central Pacific over 160^{o}E (not shown).

To compare the performance of 20 CMIP3 global models and 44 CMIP5 global models for simulating the WNP air-sea interaction, each model's produced ASI is calculated and then compared with the observation (Figure 2.1(b), (c)). Figure 2.1(b) is the averaged result of CMIP3 20 models; the observed characteristics are not represented realistically. There is no overall negative API in the WNP, but rather regions with positive API more than 0.1 is represented. Especially the core region with the strongest ASI is not captured at all. Even near 30^{o}E, where western North Pacific subtropical high (WNPSH) usually located in summer, positive API of nearly 0.3 is found. It implies that the global climate models generally produced increased precipitation in the year with higher SST, which is at odds with observations. Possible reasons why CMIP3 models fail to properly simulate the air-ocean interaction of WNP might be followings: 1) atmospheric motion is too sensitive to SST in models and 2) SST decrease due to precipitation and cloud is still poorly caught. Figure 2.1(c) is the averaged result of CMIP5 44 models. Compared to CMIP3 result, the CMIP5 ensemble has improved in some points. The ocean grid points with positive coefficients that were widely apparent in CMIP3 have decreased in CMIP5 models. Near the Philippines, even weak negative API about -0.2 is simulated. In terms of the root mean square error (RMSE) also, the CMIP5 ensemble have a better result. RMSE of CMIP3 ensemble is 0.38 and that of CMIP5 ensemble 0.33. 13.2% decreased error supports CMIP5 models' betterment. CMIP5 ensemble results, however, still far from the observation. API signals are mostly too weak over the WNP, and relatively high positive API is shown near the equator. This analysis may be appropriate to compare the model sets' overall performances. Nevertheless, it is not enough to validate the actual differences or improvements between the models because averaging all models' value can cancel out each model's result. The more reliable comparison requires proper model selection.

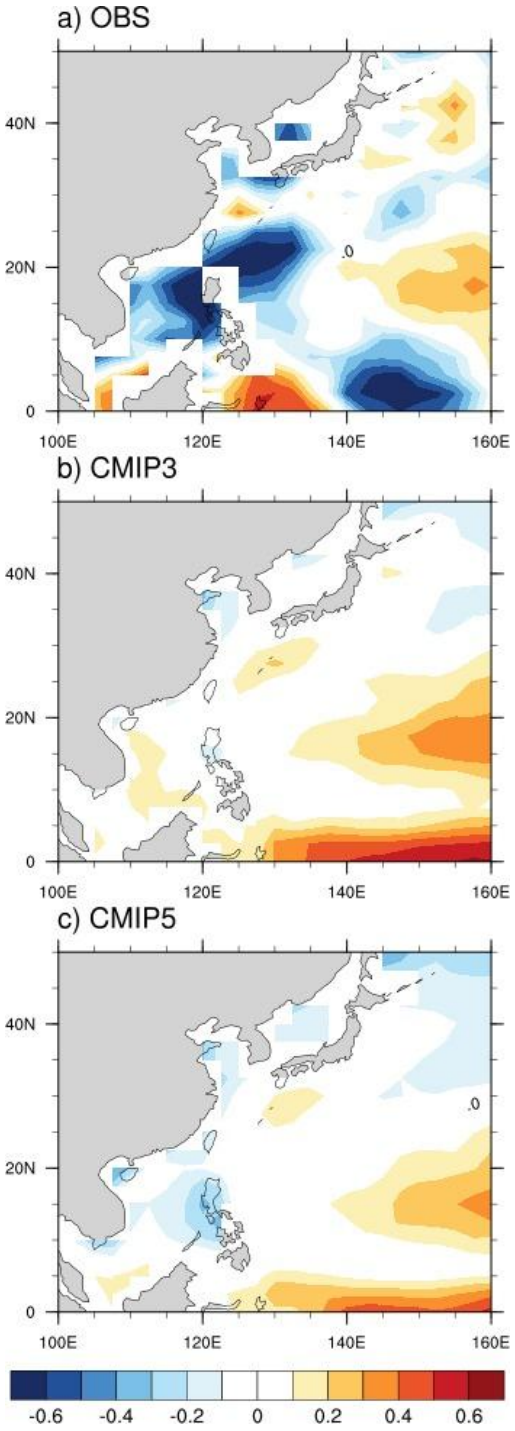

Figure 2.1. Observed (a) and simulated (b, c) ASI. The observed correlations were computed for 20 years (1980-1999) from GPCP and ERSST. The simulated results were made by the multi-model ensemble simulation of 20 CMIP3 models and 44 CMIP5 models, respectively.

Therefore, to see whether CMIP5 models are improved in simulating the WNP air-sea interaction after the model revision from CMIP3, models with good performance and models with poor performance are selected based on the API reproduction performance. Figure 2.2 lists the Taylor skill score S for API calculated by the CMIP3 and CMIP5 models in ascending order.

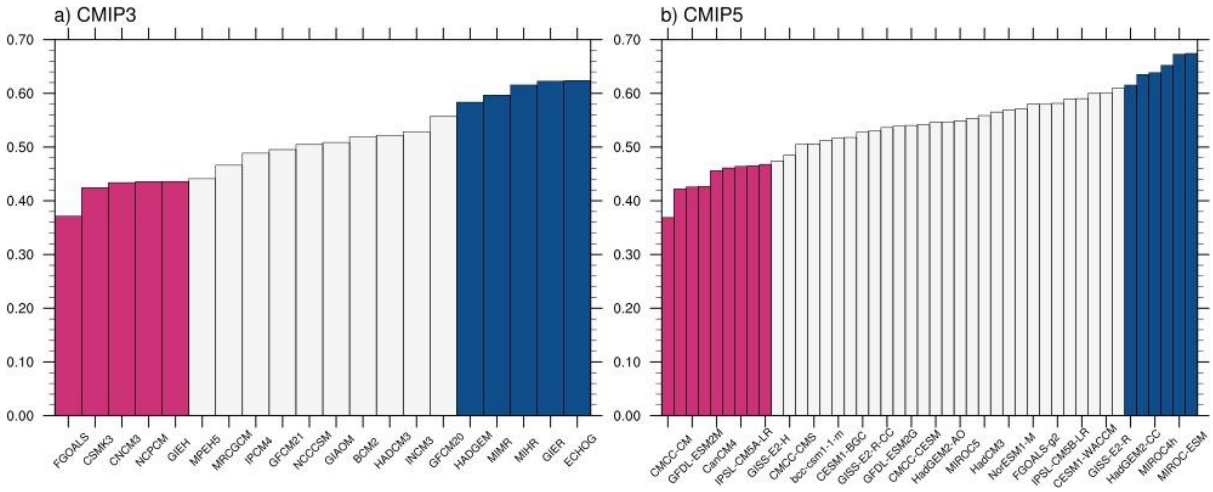

Figure 2.2. Taylor skill score of ASI calculated by (a) CMIP3 models and (b) CMIP5 models.

Models with a standard deviation of more than 1σ were selected. According to this condition, five CMIP3 good models (ECHOG, GISS-ER, MIROC3.2(hires), MIROC3.2(medres), UKMO-HadGEM1) and five CMIP3 bad models (FGOALS, CSIRO-Mk3.0, CNRM-CM3, NCAR PCM, GISS-EH) are chosen. In the same way, six CMIP5 good models (MIROC-ESM-CHEM, MIROC-ESM, CCSM4, MIROC4h, NorESM1-ME, HadGEM2-CC) and nine CMIP5 bad models (CMCC-CM, ACCESS1-3, GFDL-ESM2M, CSIRO-Mk3-6-0, CanCM4, MPI-ESM-LR, IPSL-CM5A-LR, CanESM2, GISS-E2-H) are adopted. As a result, skill score of the CMIP3 good ensemble is 0.58, and that of the CMIP3 bad ensemble is 0.39. Also, the skill score of CMIP5 good ensemble is 0.68, and that of CMIP5 bad ensemble is 0.52. Analysis of the averaged characteristics of each model set is followed. Firstly, in both CMIP3 and CMIP5 cases, the ensemble of bad models shows precipitation tends to increase as SST rises (positive ASI) in most areas in the WNP (Figure 2.3(a), (b)). It infers that warmer SST forced on increased precipitation, but induced rainfall and synoptic scale atmospheric condition can't cool SST. This is also supported with the strong ASI over 0.4 near the equator because the higher SST can trigger more convective precipitation. The difference between CMIP3 bad ensemble and CMIP5 bad ensemble is reduced positive ASI in the SCS. There shows a weak negative ASI over the west of the Philippines

in the CMIP5 bad result, where all five models of CMIP3 bad reproduce positive ASI. On the contrary, both CMIP3 and CMIP5 good model ensemble shows far more apparent negative ASI than bad model result does (Figure 2.3(c), (d)). Focused on the core region, the precipitation rate and SST are reversely correlated over the WNP. The signal is much closer to the observed value compare to the bad model ensembles. The point is that the CMIP5 good ensemble has a broader area with realistic ASI and stronger signals. All of six CMIP5 good models present negative ASI over the SCS and the south of Korea and Japan.

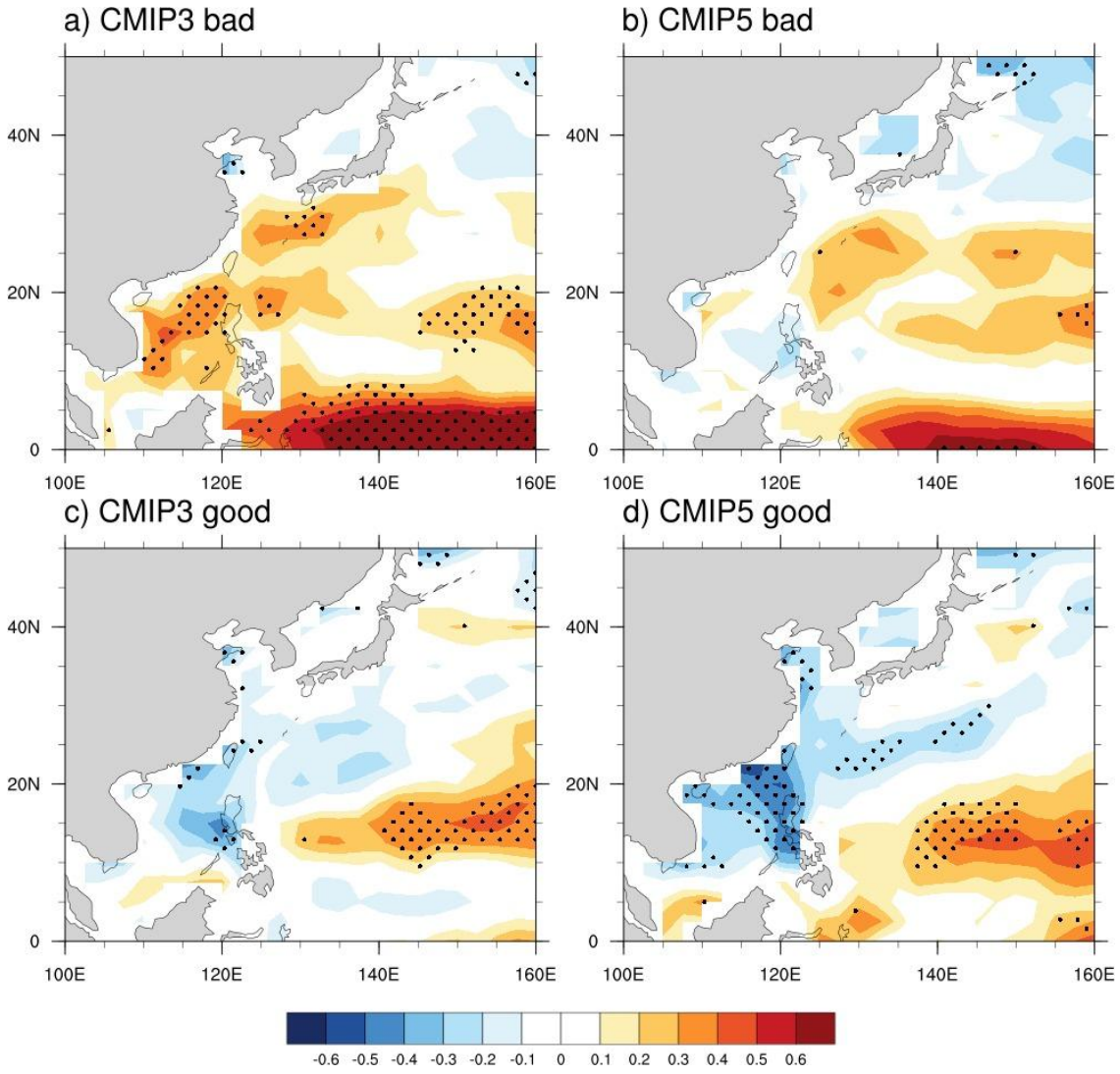

Figure 2.3. ASI between May-August (1980-1999) SST and precipitation produced by multi-model ensemble of a) CMIP3 bad models, b) CMIP5 bad models, c) CMIP3 good models, and d) CMIP5 good models.

Over the East Sea and the East of China also, strengthened negative ASI value is pronounced compared to the result of CMIP3 good models. It is regarded as the result of proper SST change due to the precipitation induced by the synoptic-scale atmospheric condition. These distinct different characteristics of good models and bad models prove that analyzing only selected members is a more suitable way to study model groups' properties. Features that were offset by each other when all 20 CMIP3 and 40 CMIP5 data are averaged are represented in Figure 2.3. The ASI of CMIP5 good models is still weak as compared with the observation. However, CMIP5 models' performance is enhanced as contrasted with that of CMIP3 models. RMSE and spatial correlation are arranged in Table 2.2. Bad ensemble's result is improved in both RMSE and spatial correlation. Spatial correlation of CMIP5 good model ensemble is higher than the bad model ensemble, but RMSE is nearly the same. However, error calculated for the core region (denoted in parenthesis) decreased in good models. In this context, it is determined that the models participating in CMIP5 have been developed compared to the CMIP3 models in terms of simulating the WNP overall air-sea interaction.

Table 2.2. RMSE and spatial correlation of ASI between the observation and simulations.

	CMIP3 bad	CMIP5 bad	CMIP3 good	CMIP5 good
RMSE	0.50 (0.61)	0.42 (0.49)	0.29 (0.33)	0.29 (0.29)
Spatial correlation	-0.20	-0.05	0.39	0.43

Chapter III

Relationship between the WNP Air-Sea Interaction and the East Asian Summer Monsoon Prediction

3-1. East Asian Summer Monsoon Simulation of CMIP5 models

The previous section identified that CMIP5 models had been upgraded concerning the WNP air-ocean interaction reproduction. Based on this, CMIP5 model results are used to analyze how the performance of simulating ASI would affect the prediction of EASM. To achieve this, selected CMIP5 good models and CMIP5 bad models are studied. Figure 3.1 shows pattern correlations and standardized deviations of precipitation produced by ensemble member of CMIP5 models. Good models simulating ASI realistically have higher pattern correlation with observed precipitation in general. Distribution in the standard deviation of models is similar in two different model sets. Good model ensemble and bad model ensemble are superior to individual models in simulating precipitation over the WNP. The performance of good model ensemble is far better than a bad model ensemble. It is understood that the ensemble result can represent the average skill of ensemble member models. Thus, comparison on good model ensemble and the bad model ensemble is conducted, analyzing precipitation and synoptic scale atmospheric features.

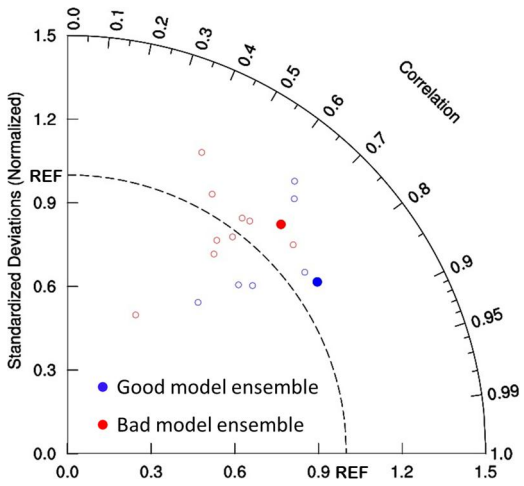

Figure 3.1. Pattern correlation and spatial standardized deviation of ratio for the seasonal (JJA) mean precipitation between observation and CMIP5 good models and (blue) and CMIP5 bad models (red) for 27 years (1979-2005).

Seasonal mean precipitation during summer (JJA) by observation and by CMIP5 models are analyzed in Figure 3.2. Climatology of observed precipitation is mainly divided into two major monsoons (Figure 3.2(a)). One is the EASM, characterized by rainfall on the area including southern China to central China, Korea, and Japan. There are two regions with a higher precipitation rate of EASM: over southern China and over south of Korea and Japan. The other monsoon is the WNPSM, which is related to heavy precipitation concentrated in the southern region below 20°N. Precipitation is mainly focused over the South China Sea (SCS) and over the tropical WNP. With these two rain bands, there is an area with little precipitation from 130°E to 160°E, which is much affected by the WNPSH. Ensemble result of CMIP5 good models shows distinct EASM and WNPSM rainfall area realistically. Overall precipitation intensity is weak compared with the observation. However, the spatial distribution of rainfall is realistic. The EASM rain-band is extending from south China to Japan; the WNPSM rain-band is well distributed over from the SCS all the way to the southwestern Philippine Sea. In addition, small rainfall domain by the WNPSM is also well captured. In contrast, ensemble result of CMIP5 bad models simulate distorted precipitation pattern. One failure is that the two major rain bands are not clearly separated from each other. Precipitation area of the WNPSM is so wide compared to the observation that the EASM rain band seems a small side branch of the WNPSM. The difference of the rainfall intensity between EASM and WNPSM is another problem. The intensity of WNPSM in the bad model ensemble is weaker than the observation, but it is comparable. Still, the intensity of EASM is simulated too weakly especially for Korea and the southern part of Japan. When it comes to RMSE, spatial correlation and Taylor skill score also, good model ensemble's performance is superior to the bad model ensemble (Table 3.1). RMSE of good models decreased by 0.56 $mm \cdot day^{-1}$ in comparison with bad models. Especially spatial correlation has a noticeable difference, indicating that spatial distribution of rain band is well captured in CMIP5 good models.

To evaluate the capacity of the good models and bad models simulating actual monsoon onset and withdrawal, validation is conducted in areas of longitude between 110°E and 130°E, where the evolution of EASM and WNPSM are revealed (Figure 3.3). Figure 3.3(a) shows the observed precipitation. From mid-May, developed precipitation passes over the SCS roughly between 15°N and 25°N. This rain band gradually goes northward and reaches over 25°N near the Yangtze river basin and southern Japan in early June. In mid to late June, the rain band has strong rainfall over the mid-latitude area. This rainfall keeps northward movement until July, making a rainy season in Korea, and dissipate. This is resulted from that the monsoon, which has expanded northeast from the Indian Ocean, moves northward along the edge of the WNPSH (Yihui and Chan, 2005). This rain band development process is a big part of the EASM. There are also rainy regions with strong rainfall in June in a lower latitude, which consists of the WNPSM.

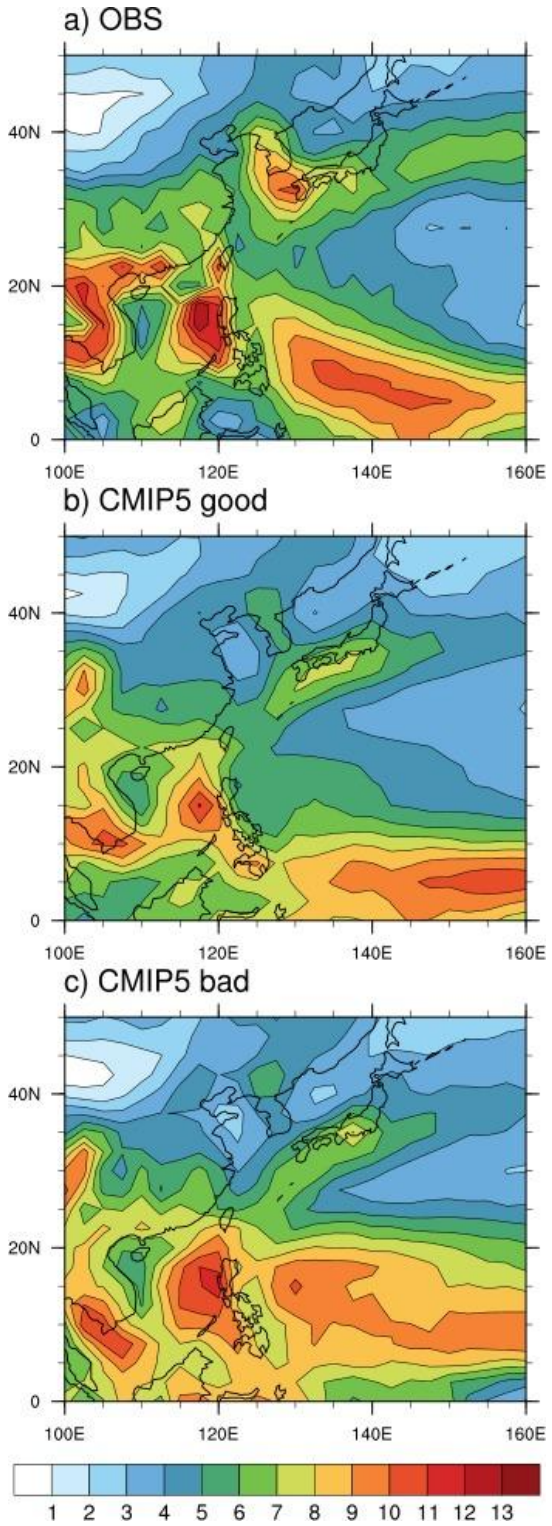

Figure 3.2. Seasonal mean (JJA) precipitation over East Asia during the summer in (a) GPCP observation, (b) CMIP5 good model ensemble and (c) CMIP5 bad model ensemble.

Table 3.1. RMSE and spatial correlation of precipitation between observation and simulations.

	Bad	Good
RMSE	1.92	1.36
Spatial correlation	0.68	0.82
Taylor skill score	0.84	0.90

The rain band locates over the southwestern Philippine Sea. The intensity gets much weaker in mid-July, but in the late July and early August, precipitation occurs again in the northeast portion of the WNP monsoon domain (10-25^{o}N). Later in September, the WNPSM rain band moves southward, but it's out of the averaged domain of this research. This analysis agrees with the monsoon rainfall peak analysis conducted by Wang (2002). CMIP5 good models realistically produced northward progress of the EASM from mid-May to early July. Rainfall focused on mid-latitude in June is also well captured. The first intense rainfall epoch of the WNPSM in June is not well reproduced, but the distinction between the EASM season and the WNPSM season is clearly seen. Although overall precipitation intensity tends to be underestimated with the good ensemble, it is known that the global climate models are likely to exhibit less precipitation strength (Dai, 2005; Stephens et al., 2010; Koutroulis et al., 2016). In contrast, CMIP bad ensemble is poor at simulating proper Asian monsoon system. First, in June, the EASM and the WNPSM are not separated from each other. Northward propagation of EASM precipitation until July, which is one of the biggest features is not produced realistically. The intensity of EASM rain is also very weak compared with that of WNPSM. In this context, the CMIP5 good model ensemble that realistically simulates the WNP air-sea interaction is also regarded as more appropriate than CMIP5 bad model ensemble to predict EASM rainfall pattern and developments. To figure out the difference in the simulated performance of precipitation, the synoptic fields of two model sets are compared with the R-2 reanalysis data (Figure 3.4). Figure 3.4(a) depicts the reanalysis geopotential height and wind vectors. During the EASM season, the WNPSH, represented by the 5880 gpm contour line, expands westward deeply. In low latitudes, westerly wind from the tropical eastern Indian Ocean is perceptible. The moist air of the Indian Ocean flows northward along the edge of the WNPSH, inducing a large amount of water vapor into the mid-latitudes.

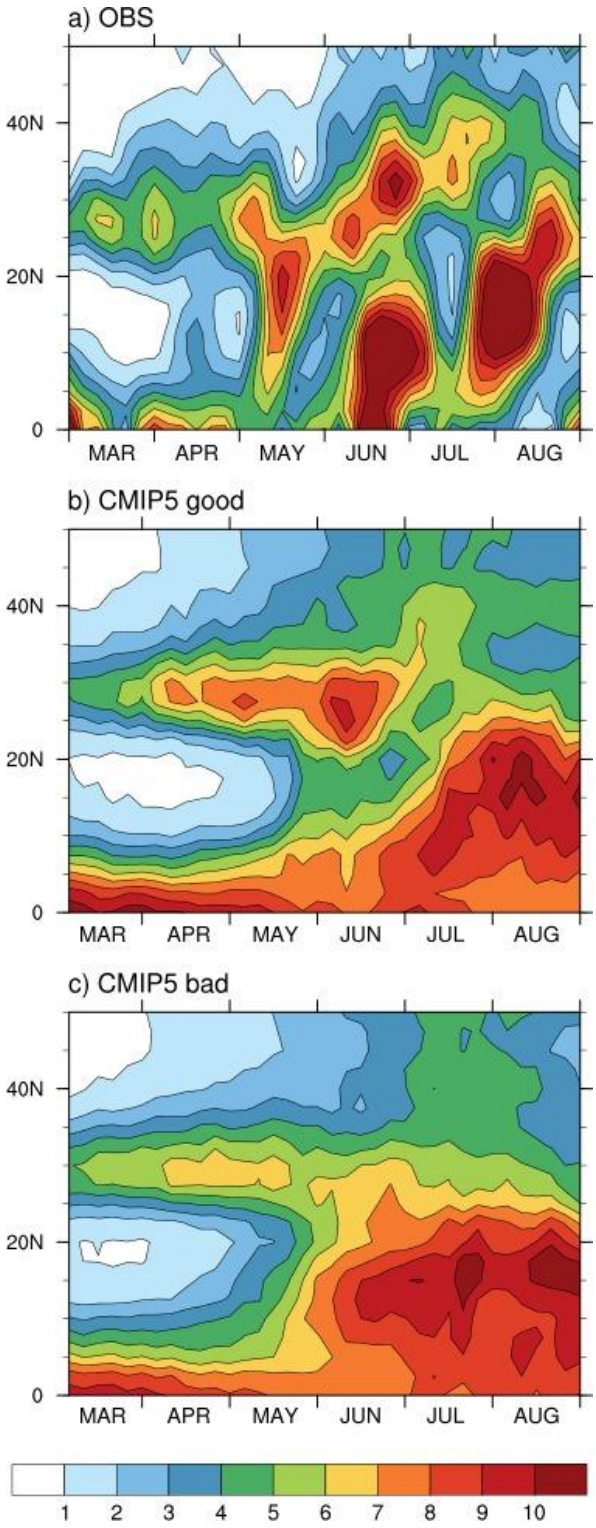

Figure 3.3. Time-latitude cross section of climatological pentad-mean precipitation on average along 100-130E°.

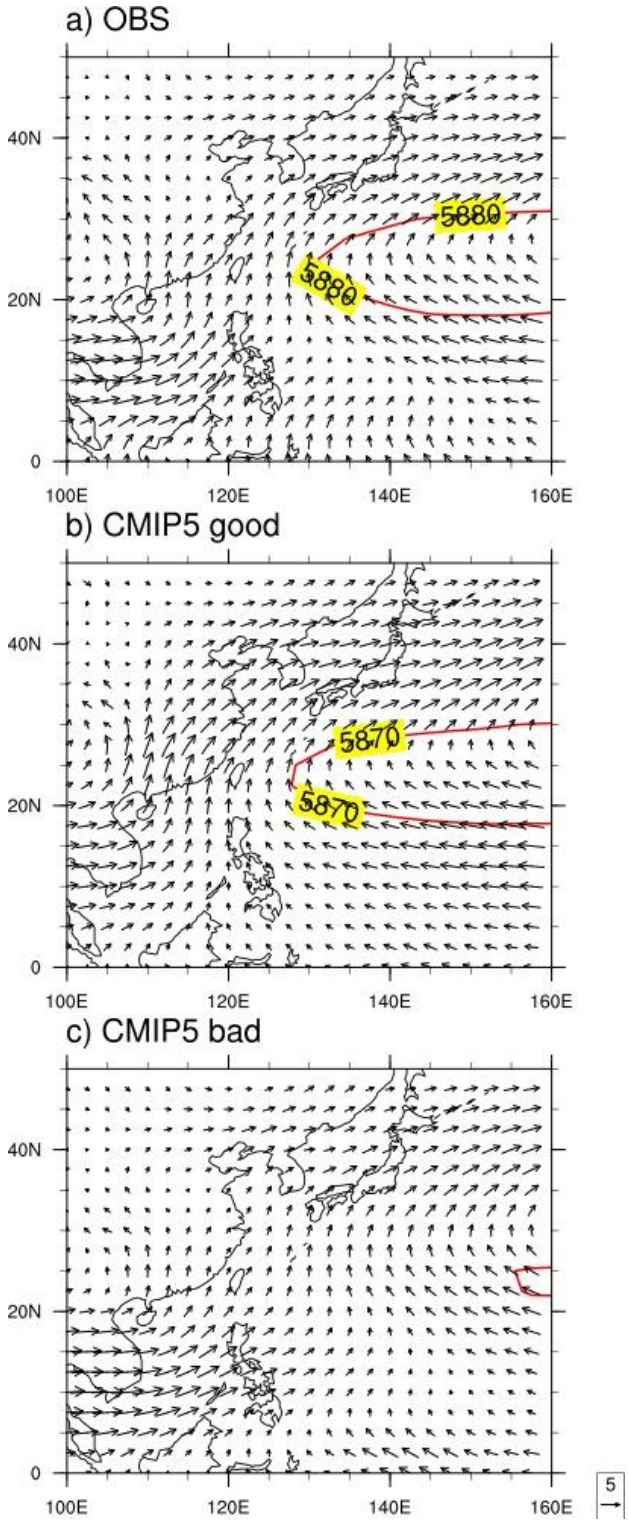

Figure 3.4. Seasonal mean (JJA) composite of 850hPa wind (vector), geopotential height (red line) of (a) R-2 reanalysis, (b) CMIP5 good model ensemble, and (c) CMIP5 bad model ensemble

Good model ensemble reasonably simulated location and strength of the WNPSH. Anticyclonic circulation over the WNP is comparably well formed, resulting in realistic westerly wind from the Indian Ocean. The wind flows northward along the WNPSH, supplying moisture into the mid-latitudes. This system is in good agreement with the R-2 reanalysis field. In contrast, bad models have flaws reproducing synoptic scale atmospheric state in monsoon season. A striking feature is that the 500-hPa geopotential height has much decreased. This weakened WNPSH can make related anticyclonic circulation weakened, resulting in intensified low-level wind. Cha et al. (2008) demonstrated that this mechanism might induce overestimated precipitation over the WNPSM domain. The strengthened low-level westerly extends to the subtropical WNP, enhancing latent heat flux from the sea surface by increasing PBL mechanical mixing in models. Figure 3.5 summarizes the physical mechanism for the WNP air-sea interaction. Convective available potential energy (CAPE) increased due to the enhanced surface latent heat flux; more active convection and overestimated precipitation may follow next.

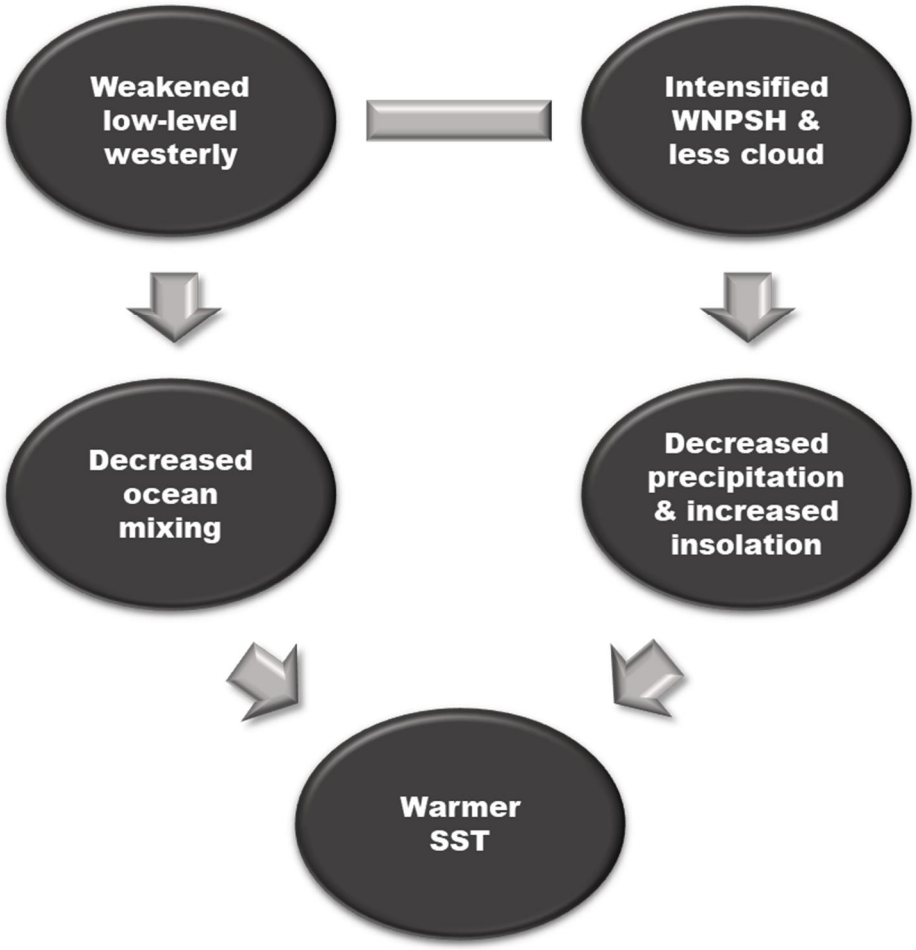

Figure 3.5. Physical mechanism for the WNP air-sea interaction occuring at the sea surface

Shrunk WNPSH is not favorable for northward wind and not sufficient to transport moisture from the eastern Indian Ocean to the mid-latitude area. As a result, precipitation is concentrated in low latitudes area, and it is difficult to produce monsoon in the mid-latitudes. This defect makes underestimated EASM in the CMIP5 bad model ensemble. In this context, the CMIP5 good models with realistic ASI is better at reproducing synoptic scale atmospheric conditions and monsoon rainfall than the bad models.

3-2. Impact of Air-Sea Interaction in the Extreme Monsoon Years

This dipole mode of East Asian summer monsoon – the EASM and the WNPSM – also has interannual variability. According to their phases, monsoon years can be divided into strong EASM years and weak EASM years. In each extreme case, different meteorological phenomena occur in East Asia and the WNP. In 1994, a representative of weak EASM years, there was record-breaking heat waves and drought during the summer monsoon season due to anomalous circulations over the East Asian-northwestern Pacific region and over the subtropical western Pacific (Park and Schubert, 1997). On the other hand, 1991 and 1998 are examples of strong EASM years. There was heavy precipitation over East Asia during summer over the Yangtze-Huaihe River Basins, making a large socio-economic loss in many countries. As aspects of two extreme monsoons are quite different, predicting strong EASM and weak EASM with higher accuracy is required. Thus, analysis on the impact of models' performance reproducing ASI on the models' skill simulating strong/weak EASM is conducted. Extreme EASM years are selected based on the Western North Pacific Monsoon Index (WNPMI) (Wang and Fan 1999; Wang et al. 2001). As the phase of the WNPSM is interannually opposite to that of the EASM, WNPMI has been considered as a qualified index also for the EASM (Kwon et al. 2005; Cha et al. 2011). Strong (weak) EASM years are defined as years with WNPMI below -0.75 sigma (above +0.75 sigma). As a result, six strong EASM years (1983, 1988, 1993, 1995, 1996, 1998) and eight weak EASM years (1981, 1985, 1986, 1990, 1994, 2001, 2002, 2004) are selected. Strong and weak EASM years by GCMs are also defined and listed in Table 3.2.

Seasonal mean (JJA) precipitation rate is different according to the seasonal variability of EASM (Figure 3.6). Observation shows that in the Strong EASM years, EASM rain band is prominently well developed from southern China to central China, Korea, and Japan, where the WNPSM is much weaker than the climatology. In weak EASM years, however, the EASM is much weaker, and the WNPSM is far stronger than in strong EASM years. Especially rainfall rate around southern Japan has a big change.

Table 3.2. Strong and weak EASM years simulated by CMIP5 good models and bad models

Model	Strong EASM years	Weak EASM years
MIROC-ESM-CHEM	1980, 1982, 1995, 1996, 1999, 2002	1984, 1985, 1987, 1988, 1992, 2000, 2003
MIROC-ESM	1984, 1988, 1991, 1997, 1999, 2001, 2002	1979, 1980, 1981, 1982, 1983, 1987, 1993, 2000, 2004
CCSM4	1987, 1993, 1994, 1995, 2002	1980, 1989, 1990, 1991, 2000, 2005
MIROC4h	1992, 1997, 2001, 2002, 2004, 2005	1985, 1987, 1990, 1991, 1993, 1994
NorESM1-ME	1982, 1993, 1997, 2000, 2005	1981, 1983, 1989, 1992, 1994, 2001
HadGEM2-CC	1987, 1990, 1997, 1999, 2001, 2002, 2005	1981, 1982, 1983, 1984, 1989, 1995, 2003
CMCC-CESM	1979, 1982, 1986, 1989, 1997, 2000, 2001, 2003	1983, 1984, 1990, 1992, 1998, 1999, 2005
ACCESS1-3	1980, 1982, 1984, 1993, 1994, 1996, 2003	1981, 1985, 1989, 1992, 1999, 2000
GFDL-CM3	1980, 1981, 1983, 1985, 1989, 1997, 1999	1979, 1991, 1993, 1996, 1998, 2002
CSIRO-Mk3.6.0	1981, 1985, 1986, 1994, 2004	1979, 1980, 1984, 1987, 1992, 1993, 2000, 2003
CanCM4	1980, 1981, 1986, 1992, 1996, 1997, 1999	1983, 1987, 1988, 1990, 1993, 1994, 2003
MPI-ESM-LR	1981, 1988, 1992, 1993, 1996, 2000	1986, 1987, 1989, 1990, 1991, 1997, 1998, 2001
IPSL-CM5A-LR	1979, 1980, 1983, 1985, 1994, 1996, 1998, 2002, 2005	1982, 1988, 1990, 1992, 1993, 1995, 1997, 2000, 2003
CanESM2	1979, 1980, 1983, 1987, 1998, 2000, 2004	1981, 1984, 1990, 1992, 2003, 2005
GISS-E2-H	1981, 1984, 1989, 1991, 1999, 2002, 2003	1983, 1987, 1994, 1995, 1998, 2000, 2004

These different aspects are reasonably reproduced with the CMIP5 good model set. Although overall rainfall intensity is weaker than the observation, EASM rain band is noticeably stronger in strong EASM years than in weak EASM years. In strong EASM years, the WNPSM rain intensity is weaker than climatology. It becomes strong in weak EASM years, and the big difference is shown over the SCS. In weak EASM years, weakened EASM precipitation is prominently captured in the good model ensemble. However, these characteristics are different from CMIP5 bad models. In bad models, intensity change of WNPSM precipitation is clearly produced. Weak EASM years have much stronger WNPSM rain band than the strong EASM years. However, EASM rain bands shape, and rainfall rate is nearly the same in Figure 3.6(e) and Figure 3.6(f). There is a slight increase in precipitation in strong EASM years near southern Japan and over the East China Sea, but it is not the difference signal of strong and weak EASM years. Thus, model ensemble, poor at producing ASI, cannot resolve the EASM precipitation and its interannual variability even though they can simulate the WNPSM. Table 3.3 is the statistics of the precipitation. Good model ensemble's performance is better than the bad model ensemble's skill both in strong EASM years and weak EASM years. Both good and bad model ensembles have a larger error with the result of strong EASM years than with the result of weak EASM years. Both biases for strong EASM years and weak EASM years are smaller in the good model ensemble are smaller than that in the bad model ensemble. It indicates that CMIP5 models are generally not good at simulating the change of the EASM rain pattern and intensity; relatively better at reproducing the WNPSM.

Figure 3.7 can explain the reason for systemic error of precipitations. In the strong EASM years, as compared with the climatology, the low-level south-westerly over East Asia is stronger, and the WNPSH is expanded further to the west. Moist air transported by the wind from the eastern Indian Ocean flows to mid-latitudes, inducing high precipitation rate in the region. The strengthened WNPSH, coexisting with the weak westerly into the tropical WNP, make reduced rainfall in South-East Asia. In weak EASM years, the low-level south-westerly is quite strong; and the WNPSH is shifted eastward compared to the climatology. This results in the weaker northward wind from low-latitude to mid-latitudes. Thus, in weak EASM years, EASM makes much more rainfall than the average precipitation, where WNPSM is far stronger. CMIP5 good models reasonably resolve these differences between the strong EASM years and the weak EASM years. Good model ensemble in strong EASM years makes realistic geopotential height and circulation, allowing enough moisture supply into the mid-latitude area. Thus EASM rain band develops sufficiently. Low-level south-westerly into the WNP is weaker than the observation, and it makes rainfall intensity over the west of the Philippines reduced. Synoptic field of the good model ensemble in weak EASM years is also similar with the observation.

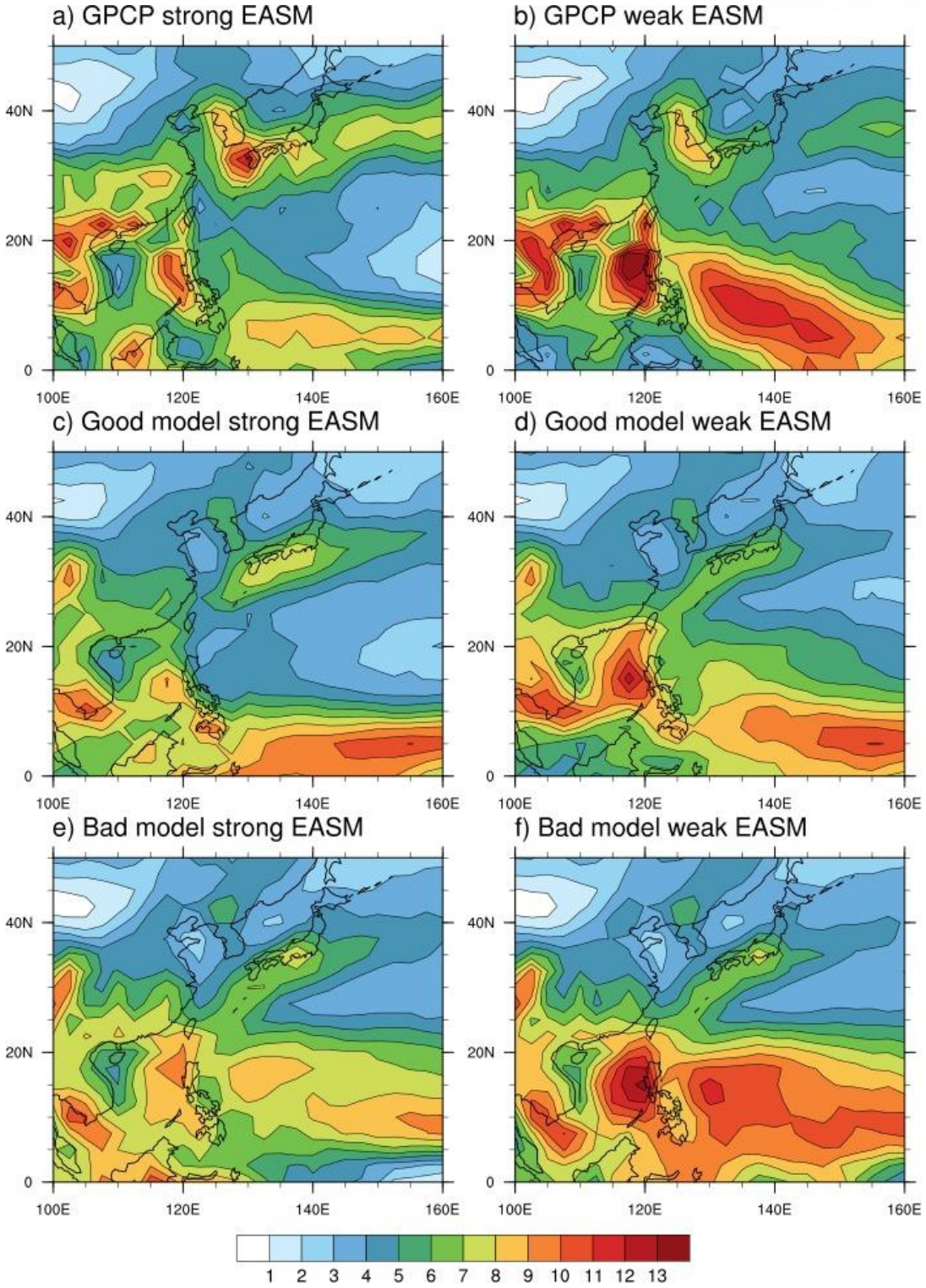

Figure 3.6. Seasonal mean (JJA) precipitation over East Asia during the summer in (a) GPCP observation strong EASM years, (b) GPCP observation weak EASM years, (c) good models strong EASM years, (d) good models weak EASM years, (e) bad models strong EASM years and (f) bad models weak EASM years.

Table 3.3. RMSE and spatial correlation of precipitation between the observation and simulations.

	Good		Bad	
	RMSE	Bias	RMSE	Bias
Strong	1.87	-0.00	2.40	0.30
Weak	1.44	0.15	2.18	0.68

Shifted 500-hPa geopotential height show that the WNPSH is much weaker than that in the strong EASM years, and the anti-cyclonic circulation on the western Pacific is also shifted rightward. More westerly wind is provided into the WNPSM region, rather than into the EASM region. On the other hand, bad model ensemble reproduces distorted synoptic-scale atmospheric conditions both in the strong EASM years and the weak EASM years. The clear WNPSH, which is supposed to locate over East Asia and WNP is not shown in the strong EASM years. Anti-cyclone related to the WNPSH is also shrunk north-eastward compared to the observation. Low-level south-westerly into the mid-latitude is also very weak, resulting in less amount of precipitation over East Asia. In weak EASM years, westerlies from the eastern Indian ocean into the WNPSM area is much strengthened as compared to in strong EASM years. It may cause much increased rainfall over the SCS and the Philippines sea. Although there are quite reasonable differences related with the WNPSM, the circulation over the EASM region have little change.

One possible reason for the overestimated precipitation is exaggerated evaporation due to the anomalous warm SST while monsoon induced rain occurs. To analyze the difference between intraseasonal variability of SST and precipitation in two extreme monsoon phases, anomaly of SST and precipitation are studied over 20-30^{o}N and 120-140^{o}E, where the WNPSH shows biggest change according to the monsoon phases (Figure 3.8). The model ensembles consist of results from four good models and seven bad models (CCSM4, NorESM1-ME, CanCM4, and GISS-E2-H are excluded due to the lack of data). To exclude seasonality of precipitation and SST, anomaly values of each variable are compared. In observation data, both strong EASM years and weak EASM years have negative ASI of -0.76 and -0.71, respectively. As high negative correlation means that the atmospheric forcing on the SST is greater than the SST's impacts to the atmosphere, atmosphere drives oceanic activity in

intraseasonal time scale as well as in interannual time scale. Good model ensemble's SST anomaly and precipitation anomaly is in inverse relation with the ASI of -0.41 and -0.55 in the strong EASM years and weak EASM years respectively. Thus, SST decrease (increase) is reasonably accompanied with the increased (decreased) rainfall in good model ensemble, which can be regarded as that atmospheric impacts are realistically works on coupled ocean models. However, in bad models, precipitation anomaly and SST anomaly are positively correlated in both strong EASM years and weak EASM years with the coefficient of 0.5 and 0.13, respectively. It implies that precipitation response is sensitive to the SST change. This phenomenon occurs mostly in the atmosphere-only models, rather than in the coupled models. Possible reason for the failure of the bad model ensemble is that there might be some problems coupling ocean models with atmosphere models, so that the SST cannot change according to the precipitation change or incoming solar radiation change.

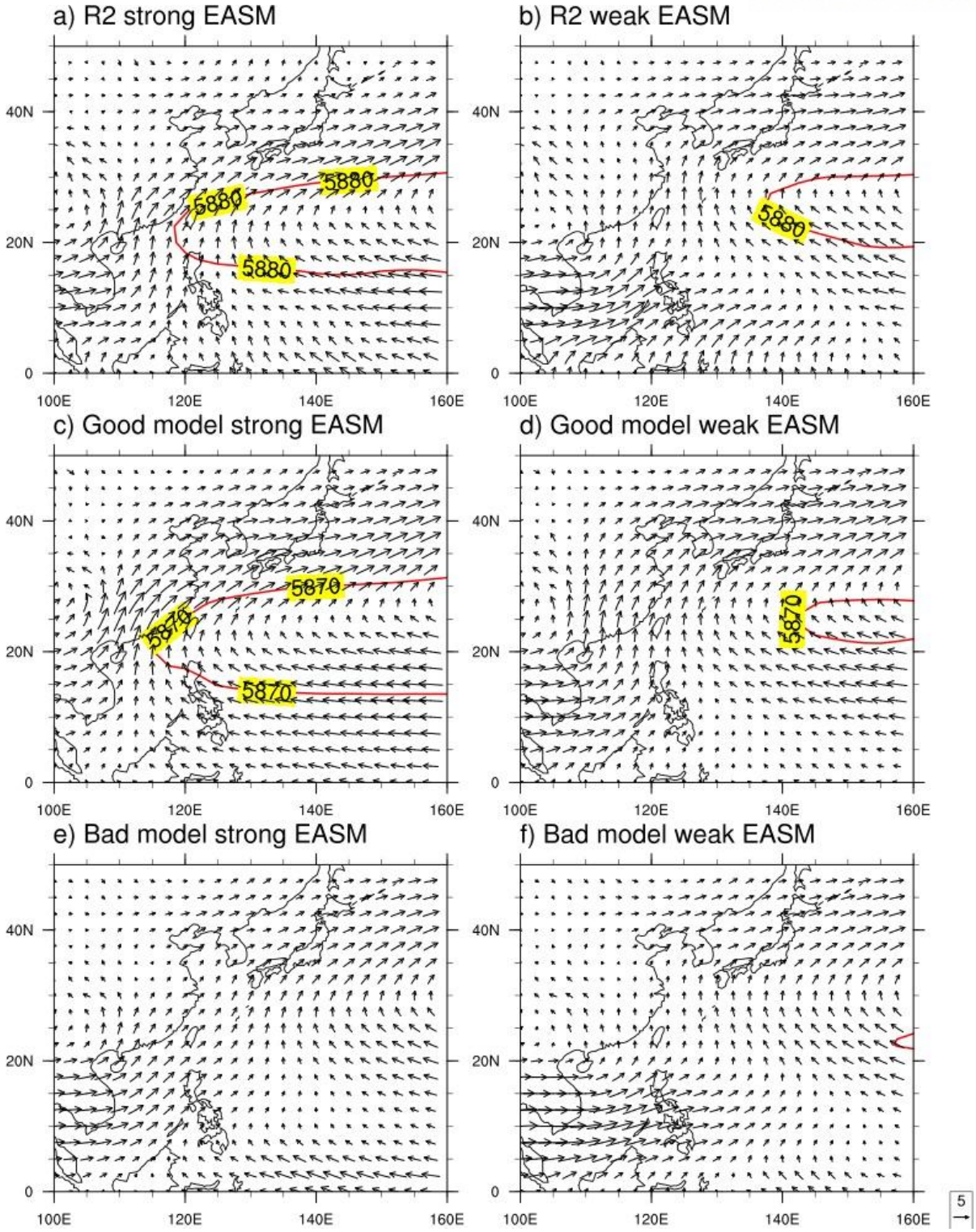

Figure 3.7. Seasonal mean (JJA) composite of 850hPa wind (vector), geopotential height (red line) of (a) Reanalysis strong EASM years, (b) Reanalysis weak EASM years, (c) good models strong EASM years, (d) good models weak EASM years, (e) bad models strong EASM years and (f) bad models weak EASM years.

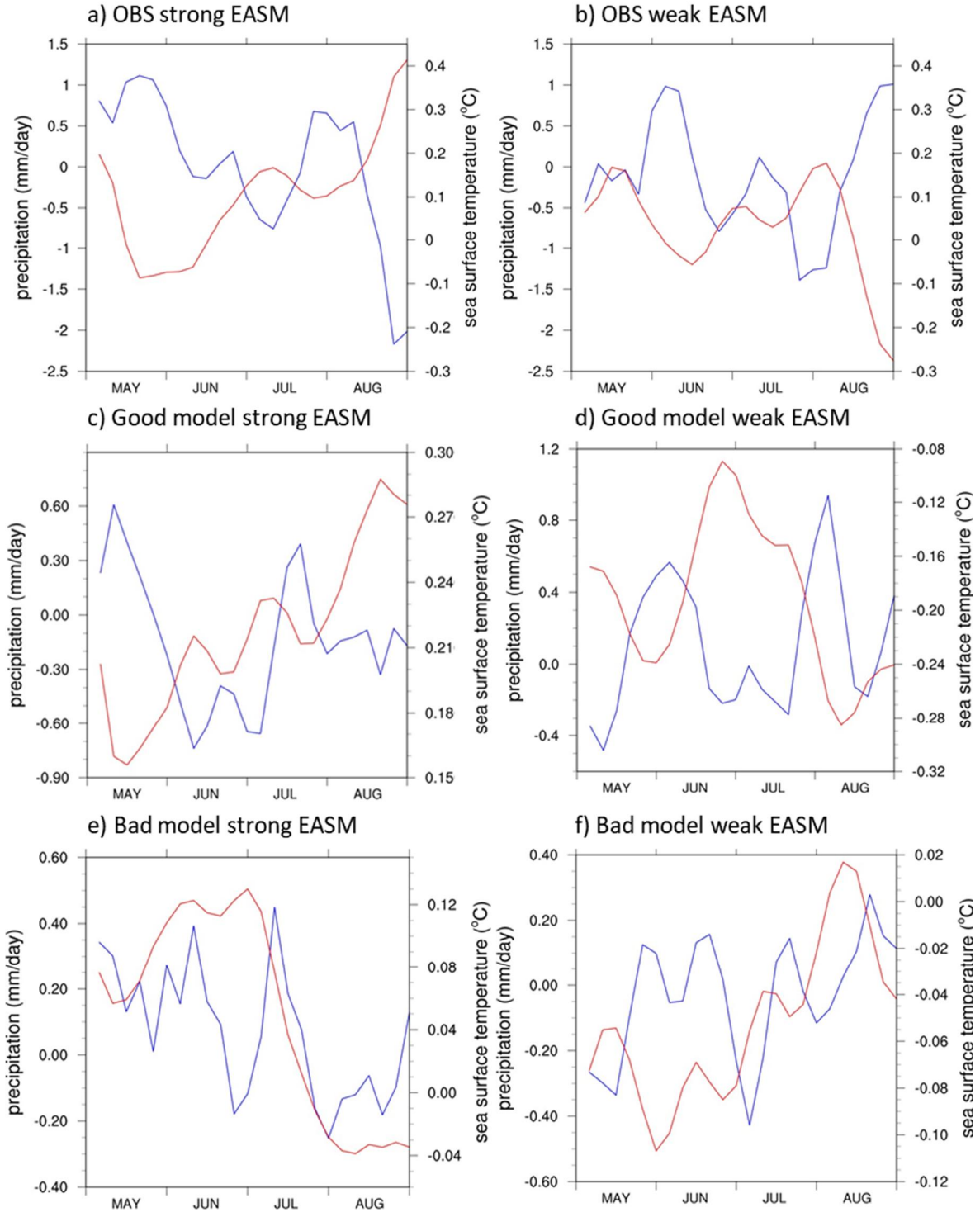

Figure 3.8. Time series of precipitation anomaly (mm·day^{-1}) and SST anomaly (°C) over 20-30oN, 120-140oE in (a) observation strong EASM years, (b) observation weak EASM years, (c) good model ensemble strong EASM years, (d) good model ensemble weak EASM years, (e) bad model ensemble Strong EASM years, and (f) bad model ensemble weak EASM years.

3-3. Future Projection of the WNP Air-Sea Interaction and EASM

Future projections of ASI for the 30-year period from 2020 to 2049 and from 2070 to 2099 over East Asia using CMIP5 good model and bad model simulations under the RCP8.5 scenario (Riahi et al., 2011) are presented in figure 3.9. The historical period is from 1979 to 2005, early future period is from 2020 to 2049, and late future period is from 2070 to 2099. In good model simulation, the overall strong negative ASI around the core region becomes weaker in the early future compared to the historical period. The ASI signal gets slightly stronger in the late future again. In bad model simulation, there are dominant positive ASI over the Philippine Sea. The ASI is bigger in the early future and gets smaller in the late future by the bad model ensemble. The difference is mostly shown over 20-30^{o}N, 120-140^{o}E. The change of ASI can be explained by the different rate of change of SST and precipitation in the future. However, ASI change does not directly indicates the increase or decrease of mean SST and precipitation over the region. Changes of mean precipitation and SST over 20-30^{o}N, 120-140^{o}E for the period from 1979 to 2099 are showed in figure 3.10. In the historical period, mean precipitation is generally decreasing, whereas SST keeps increasing. It is associated with big negative signal of ASI. In the early future simulation of good model ensemble's SST is increasing with mostly increasing precipitation. One possible reason for the phenomenon can be understood as precipitation becomes more sensitive to the SST change in the early future than in the historical period according to the increased SST due to the global warming. Precipitation and SST generally keep increasing till the end of the century. However, rate of precipitation change becomes smaller in the late future than in the early future. Weaker ASI is associated with the less precipitation increase rate. It can be interpreted that in the late future, even though SST keeps increasing, response of precipitation does not get stronger than in the early future.

In summary, with increasing SST due to the global warming, SST forcing on the precipitation can be stronger and precipitation reacts more sensitively, but in the late future, precipitation increase rate may converge to some degree, indicating that the sensitivity to SST is getting weaker. In bad model simulations' result, the changing pattern is quite similar with that in the good model simulations' result. Even though precipitation and SST already tend to increase simultaneously, the rate of precipitation increase is larger in the early future than in the historical period. It is accompanied with stronger positive ASI over the WNP. In the late future, however, precipitation increases with slower speed. It can be interpreted again, precipitation sensitivity to the SST gets stronger in the early future, and it then in gets weaker in the late future in the CMIP5 bad models.

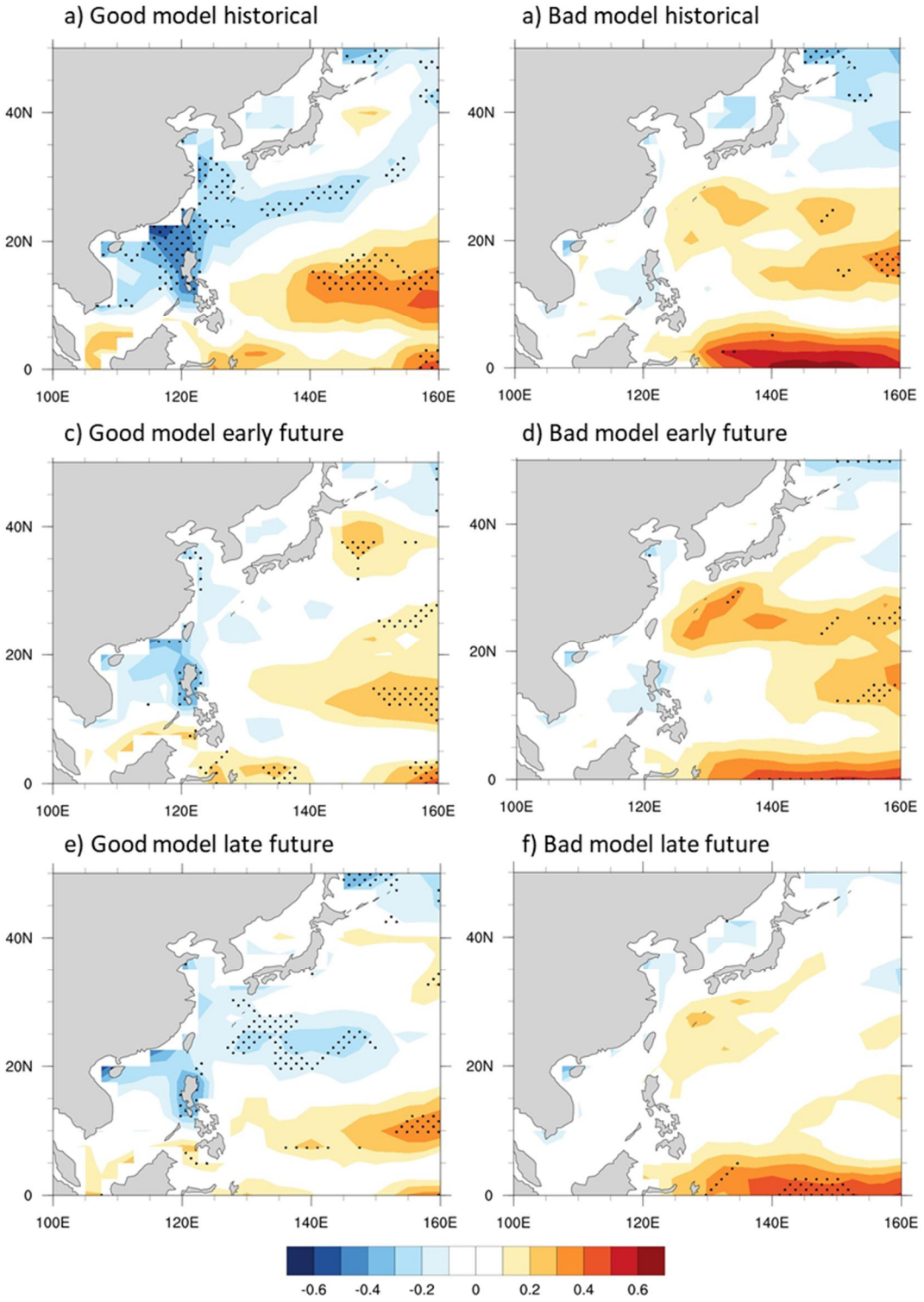

Figure 3.9. ASI between May-August SST and precipitation produced by multi-model ensemble in (a) good models historical period, (b) bad models historical period, (c) good models early future (2020-2049), (d) bad models early future, (e) good models late future (2070-2099), and (f) bad models late future.

According to this result, even though the strength of the ASI signals differ with the future period, the negative ASI is maintained in the WNP in CMIP5 good models, and it indicates that atmospheric forcing is still dominant over the WNP in the future. However, in CMIP5 bad model simulation, positive ASI is maintained from historical period to the end of twenty-first century. It can be analyzed that in bad models, the impact of SST on the precipitation keeps being dominant in the CMIP5 bad models.

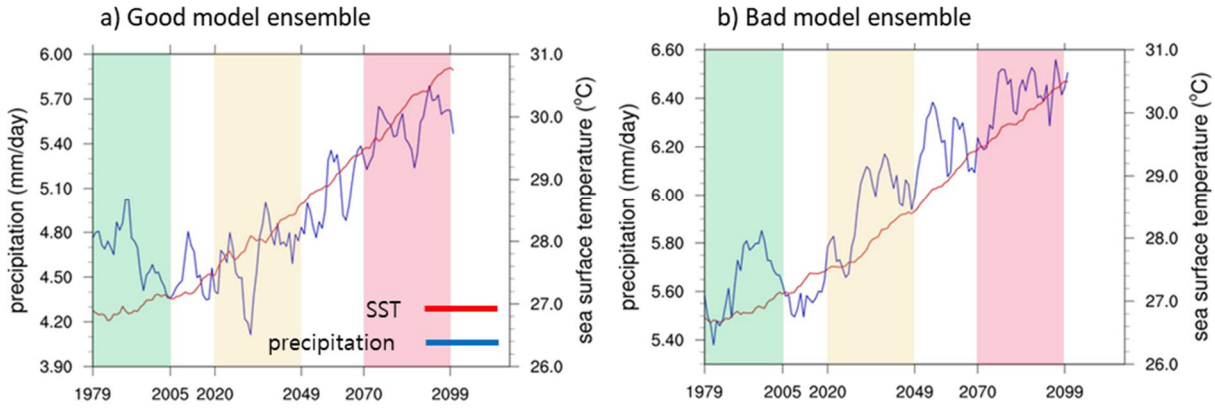

Figure 3.10. Time series of summer (MJJA) mean precipitation and SST of (a) good model ensemble and (b) bad model ensemble produced under the RCP8.5 scenario.

Figure 3.11 is summer mean precipitation over the WNP in the future. In good model simulation, precipitation increases 3.13% in the early future and 10.90% in the late future compared to the precipitation in the historical period. In bad model simulation, precipitation increases 6.69% in the early future and 17.20% in the late future. In the early future, the difference of precipitation pattern in the good models and bad models is shown mainly over the Philippine sea and near ocean basin. The difference between two model ensembles is even bigger in the late future. Even with the same future projection scenario, GCMs with different ASI simulation performance tend to produce different monsoon precipitation rate and spatial pattern. As simulation period gets longer, the difference gets bigger. Future climate projection is usually done by the ensemble of GCMs; and the future result is different according to which models are in use. Thus, in making future prediction of climate, selecting proper GCMs should be importantly considered to achieve higher accuracy and reliability.

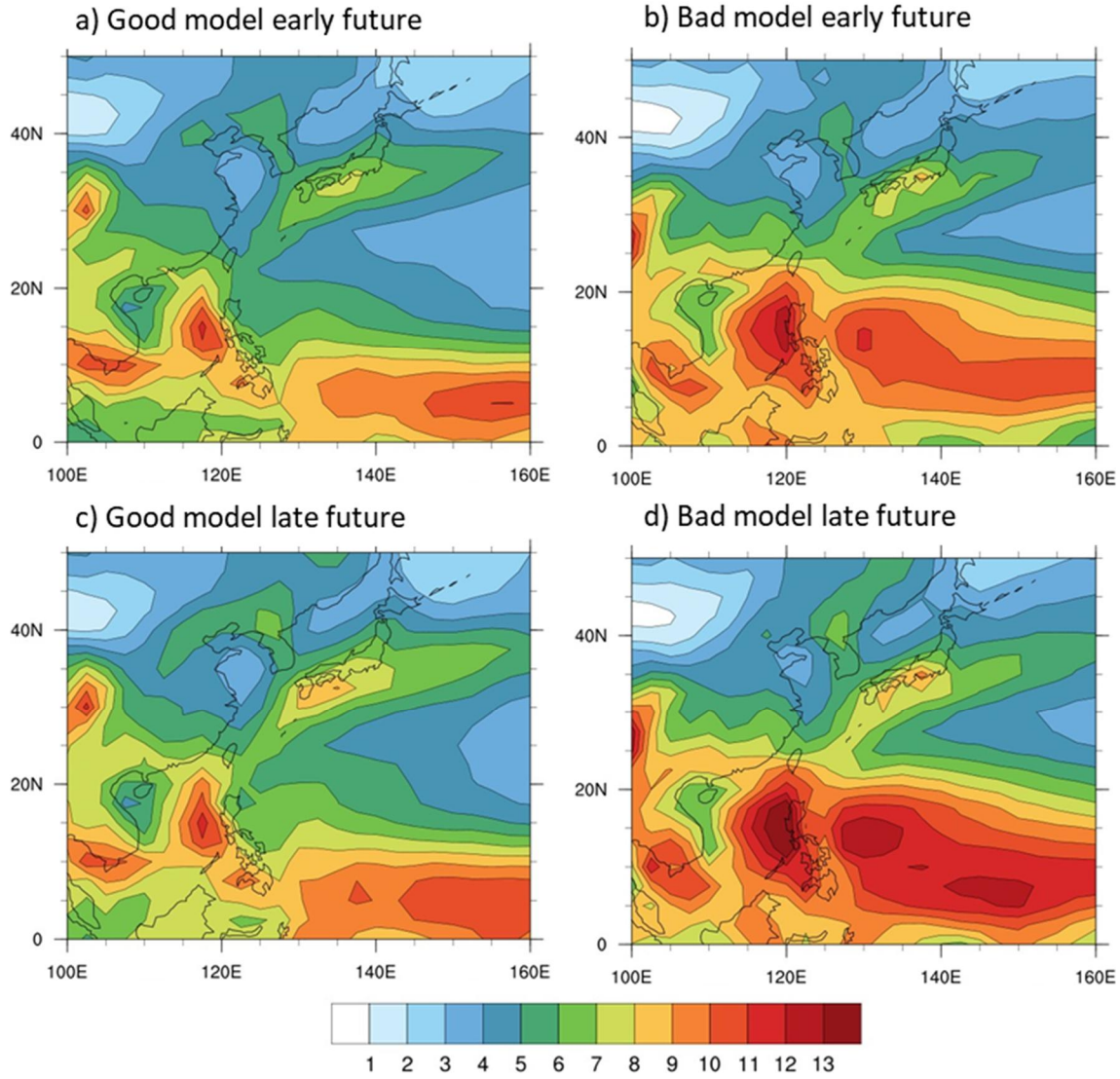

Figure 3.11. Seasonal mean (JJA) daily precipitation (mm day^{-1}) over East Asia of (a) good models in early future (2020-2049), (b) bad models in early future, (c) good models in late future (2070-2099), and (d) bad models in late future.

Chapter IV

Summary and Conclusion

In this work, a study on how the global climate models' performances reproducing EASM differ according to the performance simulating the WNP air-sea interactions. The relationship between precipitation and SST (ASI) in the WNP is different from other maritime areas at the same latitude since the atmosphere is heavily forced on the ocean. These characteristics are not realistically simulated in the atmospheric-only models, which use fixed SST. The flaw is expected to be improved in the atmosphere-ocean combined models.

To identify this theroy, evaluation and inter-comparison of CMIP3 and CMIP5 ensembles were performed first, assessing their performance in simulating the WNP air-sea interaction. The overall performance of simulating negative ASI in the WNP has improved in CMIP5 models. Particularly in CMIP5 good model results, stronger negative signals in the core region is indicated, and it implies that atmospheric forcing on the ocean is realistically simulated. The impact of air-sea interaction simulation on the performance predicting EASM are analyzed, using the improved CMIP5 model data. In good models, a realistic ASI is calculated, leading to that precipitation provides a realistic force for SST. Also, spatiotemporal characteristics of monsoon precipitation were relatively well expressed in good models than in bad models. In good models, the distribution of summer (JJA) precipitation, which is divided into EASM and WNPSM is realistically simulated, where bad models tend to underestimate the EASM domain and overestimate WNPSM domain. The synoptic field analysis shows that the WNPSH is well developed in good models, and the low-level winds in low-latitudes are also adequately produced. In bad models, however, the EASM is not fully developed as the low-level westerly wind is overestimated and water vapor is not actively supplied to mid-latitudes due to the collapse of the WNPSH. CMIP5 good models with realistic ASI simulation are also good at simulating interannual variability of EASM as well as seasonal mean rainfall. Rain band's location and intensity far closer to the observation, where bad model ensemble makes impractical EASM inter-annual variability. Changes of WNPSM between the strong EASM years and the weak EASM years are well detected by good model ensemble; and somewhat realistically produced in bad model ensemble too. It is concluded that the global climate models have different EASM simulations depending on the performance simulating air-sea interaction in the WNP. A model that realistically considers the feedback that rainfall gives to SST in the WNP can predict the spatial and temporal distribution of the EASM. Thus, it has been proved that the lack of the forces that the atmosphere imposes on the ocean may be the reason why the global climate model fails to reproduce the EASM properly.

Based on the analysis, future projection of WNP air-sea interaction is conducted under the RCP 8.5 scenario. Compared to the historical period (1979-2005), early future (2020-2049) and late future (2070-2099). In both good models and bad models, precipitation and SST increase in the early future, and increase in larger amount in the late future. However, different rate of increase of precipitation and SST are accompanied with different aspects of ASI change in the early future and late future over the WNP. Good model simulation in the early future, overall negative ASI gets weaker, for the precipitation tends to increase sharply in the early future. However, the ASI gets stronger in the late future of good simulation as precipitation increasing rate is smaller than in the early future. Still, the signal is weaker than the value in the historical period. Bad model simulation simulated positive ASI over the WNP continuously, but with different strength according to the precipitation and SST change rate. The positive ASI gets stronger in the early future, as precipitation is increasing rapid with increasing SST, but the signal gets weaker in the late future, because the precipitation increase is weaker compared to that in the early future. The weakened positive ASI signal is even weaker than that in the historical period. GCMs with different performance simulating the WNP air-sea interaction produce precipitation of different characteristics. Both in early future and in late future overall precipitation in the bad model simulation is larger than that in the good model simulation. Thus, projection of future precipitation would vary in intensity and spatial pattern according to the selected GCMs. As the result of the future precipitation projection is different in a great degree according to the model, selection of GCMs requires making careful standards for proper prediction of future climate.

The study evaluated the simulated performance of CMIP5 models for the WNP air-sea interaction and identified elements of global climate models that need to be developed to predict the EASM. This can contribute to an understanding of the WNP atmospheric phenomena using CMIP5 models and can help with direct performance comparisons between the models. The fundamental causes of differences in the simulating air-sea interaction on the WNP by CMIP5 models are not dealt with in this research. To overcome this limit, models' physical characteristics and sensitivities between internal variables that affect the model performance need to be identified further.

Chapter V

References

Adler, R. F., Huffman, G. J., Chang, A., Ferraro, R., Xie, P. P., Janowiak, J., ... & Gruber, A. (2003). The version-2 global precipitation climatology project (GPCP) monthly precipitation analysis (1979–present). Journal of hydrometeorology, 4(6), 1147-1167.

Cha, D. H., Jin, C. S., & Lee, D. K. (2011). Impact of local sea surface temperature anomaly over the western North Pacific on extreme East Asian summer monsoon. Climate dynamics, 37(9-10), 1691-1705.

Cha, D. H., Lee, D. K., & Hong, S. Y. (2008). Impact of boundary layer processes on seasonal simulation of the East Asian summer monsoon using a regional climate model. Meteorology and Atmospheric Physics, 100(1-4), 53-72.

Cha, D. H., Jin, C. S., Moon, J. H., & Lee, D. K. (2016). Improvement of regional climate simulation of East Asian summer monsoon by coupled air–sea interaction and large scale nudging. International Journal of Climatology, 36(1), 334-345.

Dai, A. (2006). Precipitation characteristics in eighteen coupled climate models. Journal of Climate, 19(18), 4605-4630.

Fu, X., & Wang, B. (2004). Differences of boreal summer intraseasonal oscillations simulated in an atmosphere–ocean coupled model and an atmosphere-only model. Journal of Climate, 17(6), 1263-1271.

Fu, X., Wang, B., & Li, T. (2002). Impacts of air–sea coupling on the simulation of mean Asian summer monsoon in the ECHAM4 model. Monthly weather review, 130(12), 2889-2904.

Gadgil, S., & Sajani, S. (1998). Monsoon precipitation in the AMIP runs. Climate Dynamics, 14(9), 659-689.

Kanamitsu, M., Ebisuzaki, W., Woollen, J., Yang, S. K., Hnilo, J. J., Fiorino, M., & Potter, G. L. (2002). Ncep–doe amip-ii reanalysis (r-2). Bulletin of the American Meteorological Society, 83(11), 1631-1644.

Kim, E. J., & Hong, S. Y. (2010). Impact of air sea interaction on East Asian summer monsoon climate in WRF. Journal of Geophysical Research: Atmospheres, 115(D19).

Koutroulis, A. G., Grillakis, M. G., Tsanis, I. K., & Papadimitriou, L. (2016). Evaluation of precipitation and temperature simulation performance of the CMIP3 and CMIP5 historical experiments. Climate Dynamics, 47(5-6), 1881-1898.

Lau, K. M., Kim, K. M., & Yang, S. (2000). Dynamical and boundary forcing characteristics of regional components of the Asian summer monsoon. Journal of Climate, 13(14), 2461-2482.

Lu, R., & Lu, S. (2014). Local and remote factors affecting the SST–precipitation relationship over the western North Pacific during summer. Journal of Climate, 27(13), 5132-5147.

Meehl, G. A., Boer, G. J., Covey, C., Latif, M., & Stouffer, R. J. (2000). The coupled model intercomparison project (CMIP). Bulletin of the American Meteorological Society, 81(2), 313-318.

Meehl, G. A., Covey, C., Delworth, T., Latif, M., McAvaney, B., Mitchell, J. F., ... & Taylor, K. E. (2007). The WCRP CMIP3 multimodel dataset: A new era in climate change research. Bulletin of the American Meteorological Society, 88(9), 1383-1394.

Park, C. K., & Schubert, S. D. (1997). On the nature of the 1994 East Asian summer drought. Journal of climate, 10(5), 1056-1070.

Riahi, K., S. Rao, V. Krey, C. Cho, V. Chirkov, G. Fischer, G. Kindermann, N. Nakicenovic, and P. Rafaj (2011), RCP8.5—A scenario of comparatively high greenhouse gas emissions, Clim. Chang., 109,33–57.

Seo, K. H., Ok, J., Son, J. H., & Cha, D. H. (2013). Assessing future changes in the East Asian summer monsoon using CMIP5 coupled models. Journal of Climate, 26(19), 7662-7675.

Stephens, G. L., L'Ecuyer, T., Forbes, R., Gettelmen, A., Golaz, J. C., Bodas Salcedo, A., ... & Haynes, J. (2010). Dreary state of precipitation in global models. Journal of Geophysical Research: Atmospheres, 115(D24).

Taylor, K. E. (2001). Summarizing multiple aspects of model performance in a single diagram. Journal of Geophysical Research: Atmospheres, 106(D7), 7183-7192.

Taylor, K. E., Stouffer, R. J., & Meehl, G. A. (2012). An overview of CMIP5 and the experiment design. Bulletin of the American Meteorological Society, 93(4), 485-498.

Tompkins, A. M. (2001). On the relationship between tropical convection and sea surface temperature. Journal of climate, 14(5), 633-637.

Wang, B. (2002). Rainy season of the Asian–Pacific summer monsoon. Journal of Climate, 15(4), 386-398.

Wang, B., Ding, Q., Fu, X., Kang, I. S., Jin, K., Shukla, J., & Doblas Reyes, F. (2005). Fundamental challenge in simulation and prediction of summer monsoon rainfall. Geophysical Research Letters, 32(15).

Yihui, D., & Chan, J. C. (2005). The East Asian summer monsoon: an overview. Meteorology and Atmospheric Physics, 89(1-4), 117-142.

Acknowledgement

This work was funded by the Korea Meteorological Administration Research and Development Program under Grant KMI(KMI2018-01211)

감사의 글

연구자로서 내디딘 첫걸음인 석사과정을 마무리하며, 그 길을 응원해주시고 제 부족한 한 걸음 한 걸음에 도움을 주신 많은 분께 큰 감사를 표합니다.

전공을 바꾸면서 어려움을 겪던 학부 3학년부터 석사 졸업을 이룰 때까지 5년이라는 긴 시간 동안 늘 든든히 이끌어 주신 차동현 교수님, 진심으로 감사드립니다. 첫 인턴 신청을 위해 오피스 문을 두드리던 그 순간은 어쩌면 제 유니스트 생활 가운데 가장 큰 기회였는지 모릅니다. 격려하실 때는 자상하게, 조언을 주실 때는 단호하게, 또 칭찬과 응원하실 때는 세상에서 가장 기쁘게 대하시는 교수님을 만나게 되어 저는 학생으로서, 또 한 인간으로서 많이 성장하였습니다. 교수님께서 들이신 많은 시간이 헛되지 않도록 앞으로도 노력하여 더 나은 사람이 되겠습니다. 정말 감사합니다.

제 학위논문을 위해 지도해주시고, 시간을 내어주신 이명인 교수님과 송창근 교수님께 감사의 말씀을 드립니다. 바쁘신 와중에도 제 연구가 더 발전할 수 있도록 도움을 주신 덕분에 저는 연구를 진행하는 방법과 연구자로서 나아가기 위한 태도를 배울 수 있었습니다.

오랜 시간 함께했던 재해기상 연구실원들에게도 깊이 감사드립니다. 박창용 박사님. 넘치는 에너지로 늘 북돋아 주시고, 질문드릴 때마다 반기며 알려주셔서 정말 많은 도움이 되었습니다. 감사합니다. 연구실의 든든한 대들보인 연구원 오빠들. 항상 고생해주시는데 제대로 표현도 못 하고, 의지만 한 것 같아 죄송한 마음도 듭니다. 늘 감사히 생각하고 있습니다. 연구실 초기부터 이렇게 자리 잡기까지 함께 고생한 선배, 하나뿐인 동기, 그리고 지금의 저보다도 훨씬 잘해주고 있는 후배들에게 정말 감사하다고 전하고 싶습니다. 연구실원들의 노력과 열정 덕분에 앞으로도 우리 재해기상 연구실이 더 단단히 성장할 것이라고 믿습니다. 이 짧은 글을 통해 제 마음이 전달되기를 바랍니다. 멀리서 늘 응원하고 있겠습니다.

졸업을 함께하며 같이 고생한 친구들. 혼자 걸었더라면 너무나 힘들고 어려웠을 이 길을 함께해줘서 정말 고맙습니다. 이제 더 나은 시간을 보내게 되어 정말 축하하고, 같이 보낸 이 힘든 시간이 큰 추억이 되어 나중에 웃으며 이야기할 수 있기를 바랍니다.

언제나 제일 큰 힘이 되어주는 가족. 가장 사랑하고 감사합니다. 어려울 때도 끝까지 저를 믿어주시고 따뜻한 밥으로 응원해주신 부모님 덕분에 석사라는 학위를 마무리할 수 있었습니다. 두 분의 노력과 사랑으로 이만큼 자랐습니다. 그 깊은 마음을 갚을 길이 있을지 모르지만, 더 큰 사랑으로 보답하고 싶습니다. 마지막으로, 애써 신경 쓰지 않아도 맡은 자리에서 큰일 해내고 있는 사랑하는 두 동생에게 감사를 전합니다.